General remarks:

Review of acp-2019-397: "A revisit of parametrization of summer downward longwave radiation over the Tibetan Plateau from high temporal resolution measurements" by Liu et al. This paper uses high temporal resolution measurements to evaluate the existing downward longwave radiation (DLR) parameterizations under clear-sky, cloudy and overcast conditions at the Tibetan Plateau (TP). The authors have done a good job in the literature review and the data is valuable. The careful discrimination of clear sky is also meaningful. However, this manuscript does not report significant advances nor novel aspects of experimental and theoretical methods and techniques. The major conclusions, such as the best DLR parameterization scheme that is suitable for TP have been reached by other researchers, such as Zhu et al 2017, as mentioned in the paper.

Reply: We greatly appreciate the reviewer's efforts on reviewing our manuscript.

Yes, DLR parameterization has been widely studied across the world, even including DLR in the TP. It should be noted that most parameterizations are based on hourly measurements of DLR and meteorological variables, such as Zhu et al., (2017) and Wang and Liang, (2009). Our major point is that clear-sky DLR parameterization may be seriously impacted by clear-sky data samples that are very likely contaminated by cloud residuals if human observations of cloud or hourly DLR measurements are used as the unique criteria in selecting data samples. Our result (Figure 3) clearly showed that clear-sky DLR in the previous studies was very likely overestimated by cloud residuals, which would significantly affect studies that take the clear-sky DLR estimation as their prior requirement, for example, cloud DLR forcing. Moreover, we studied the relationship between cloud base height and DLR that has never been investigated in the TP before. We consider these are our original contributions to our understanding of DLR parameterization in the TP. This research would be not possible if a comprehensive measurement project had not been performed. As one of important parts of a cooperated field campaign, the state-of-the-art pyranometer and pyrgeometer with ventilation and heating system are used to respectively measure downward shortwave and longwave radiation with 1-minute resolution, in addition, Lidar measurements provide much more information about clouds than before. To our best knowledge, installation of radiometers and Lidar site by site has never been performed, furthermore, 1-minute measurements are very rarely reported in the TP. These should be our novel aspects of experimental method, which indeed favors for our DLR parameterization study.

The detailed comments are listed below.

Major Comments:

1. Improved DLR estimation: In the abstract, as well as in Ln 353, the authors state that the DLR estimation is notably improved after local calibration. I think this statement is misleading. The authors use existing parameterizations to fit the data measured at TP. And for sure, the same fitting equation but with different coefficients would give better results compared with the literature parameterization that uses coefficients derived from measurements conducted at different places or at different conditions.

Reply: Many DLR parameterizations have been created based on local collocated DLR and meteorological data in the literatures. Application of these methods to every specific location generally includes two aspects. The first is to select the best parameterization formula that is most suitable for the local condition. The second is to derive local coefficients based on collocated DLR and meteorological observations. We tested a few widely used parameterizations and recommended one parameterization with the best performance that is able to improve the DLR estimation in the TP. We modified our manuscript according to these considerations as follows.

Comparing to previous studies, DLR parameterizations here are shown be characterized by smaller root mean square error (RMSE) and higher coefficient of determination (R^2).

2. Different parameters with Zhu et al (2017): Were the datasets of DLR, e, and T used in this manuscript measured at the same time and same sites compared with Zhu et al 2017? Otherwise, it might not be appropriate to say the difference is caused by cloud contamination (Ln 321-324). The difference can also be caused by different DLR magnitudes.

Reply: Data of DLR, e, and T used in our study are not same in time or site as those used by Zhu et al. (2017). Hourly measurements are used by Zhu et al. (2017) but we use 1-mintue measurements. Our major point is that caution should be paid to the DLR parameterizations based on hourly or daily DLR and meteorological measurements. Data used in Zhu et al. (2017) are not available to us. We only take the parameterization formula recommended by Zhu et al. (2017) to compare our clear-sky measurements and parameterization. Different DLR measurements may contribute to the difference in clear-sky parameterization, however, we tend to suggest that it is very likely contaminated by residual cloud contamination based on the following reasons. First, in Figure 3, mean DLR values from measurements, our parameterization and Zhu et al. formula are 268.6±19.7 Wm^{-2}, 268.7±19.4 $W.m^{-2}$, and 295.0±18.4 $W.m^{-2}$, respectively. The result from Zhu et al. exceeds the measurements by 25 $W.m^{-2}$ (10%), that is much more than the expected uncertainty of the measurements (2.5% or 4 $W\ m^{-2}$) (Stoffel, 2005). This implies that different measurements cannot explain this large systematic bias. Second, the method of clear–sky identification in Zhu et al (2017) based on the DLR observation (Marty and Philipona, 2000) has its potential shortcoming. This method had been further assessed by Sutter et al. (2004) who stated that “the thin high cloud” can be misclassified as clear sky. More important, comparison of cloudy DLR parameterizations between this study and Zhu et al. (2017) showed good agreement (Figure below). Therefore, we tend to think that cloud residuals should be the major contributor to the difference. We discuss this issue in the revised manuscript.

Minor Comments:

1. Ln 27: ‘highly sensitive’—-‘high sensitivity’

Reply: Done, thanks.

2. Ln 34: ‘by making maximal use of’—-‘by making the maximal use of’

Reply: We revised this sentence as follows

Three independent methods are used to discriminate clear sky from clouds based on 1-minute downward shortwave, longwave radiation measurements as well as Lidar data.

3. Ln 63: What is the ‘2-sigma uncertainty of DLR measurement’?

Reply: sigma here means standard deviation, if the distribution of uncertainty of measurements is taken be Gaussian, 2-sigma uncertainty means the uncertainty of 95.5% of measurements is within this range.

4. Ln 120: ‘would expected’—-‘would be expected’
Reply: Done, thanks.
5. Ln 141: ‘since 2011’——Did you mean in 2011?
Reply: We use the same instruments in these 3 stations. The measurements are made in summer, 2011 in NQ, 2014 in NC, and 2016 in AL.
6. Ln 153: What the specific measurement periods for the three stations are?
Reply: Information is presented in Table 1. We omit this information to keep the text concise.
7. Ln 156: The authors give detailed description of CG4. How about CM21?
Reply: CM21 is a high performance research grade pyranometer. It uses the same detector as CM11 that is used by many studies, but introduction of individually optimized temperature compensation for CM21 makes it having much a smaller thermal offset than CM11.
8. Ln 269: ‘. Both used T: : :’—-‘both used T: : :’
Reply: Done, thanks.
9. Ln 282: Add reference for k-fold cross-validation method.
Reply: Done, thanks.
10. Ln 369: Can you give examples of the ‘specific meteorological and cloud conditions’?
Reply: CRE variation increases from 25 to 50 $W\cdot m^{-2}$ as CBH increases because water vapor influence and its variation goes up.
11. Ln 371-372: What is the supporting evidence for the ‘fact that that clouds in the TP with the same CBH as that in Girona have relatively lower temperature’?
Reply: This is because the altitude of stations in the TP is much higher than that in Girona. We comment on this in the revised manuscript.
12. Equations in this manuscript should be followed by definitions of each parameter and corresponding units.
Reply: Done, thanks.

General Remarks.

The parameterizations used to calculate DLR are pretty outdated, as stated in the introduction and other places in this study. One question is that the empirical parameterizations, for example those used in this study, are strongly dependent on locations and time and thus might be suitable for specific locations and seasons but not for others. As the authors stated in introduction 'Understanding of complex spatiotemporal variation of DLR and its implication is essential for improving weather prediction, climate simulation as well as water cycling modeling'. The empirical parameterizations are apparently not able to obtain complex spatial-temporal variations of radiation flux. Actually, an accurate radiation transfer model would be a better choice to calculate radiation flux. Cloud optical properties, especially cloud optical depth is critical to modulate radiation flux, which unfortunately has not taken into account in this study. Also, a simple way is used to calculate cloud fraction (equation 1) in the manuscript, so it is necessary to evaluate the calculated values with the observed ones at the meteorological site over TP.

Reply: We greatly appreciate the reviewer's opinions on our submission. We revised the manuscript according to these comments and suggestions.

Yes, not only DLR but also any radiation flux can be calculated from an accurate radiative transfer model if information about atmospheric radiatively active compositions is well known, but unfortunately, our knowledge of these radiatively active compositions are very limited under many circumstances. Regarding DLR estimation in specific, information about cloud amount, type, phase, height is more or less related to DLR, let it alone remarkable effects of water vapor content and its profile under clear sky condition on DLR. Much progress has been made on DLR derivation from satellite measurements, however, satellite remote sensing DLR products are still not free of large uncertainty (Zhou et al., 2007; Ahn et al., 2018), especially in the regions of elevated or complex terrain. As pointed out by the reviewer, the empirical parameterizations have limitation, but their advantages are also apparent. The method is simple but effective in the estimation of DLR, especially in regions with the parameterizations locally adjusted by high quality DLR measurements. Moreover, meteorological variables used for the DLR estimation are available across the world. These apparent advantages make this method is still widely used by the community and contribute to our understanding of the energy budget of the Earth's system (Wang et al., 2013).

Cloud optical depth is a key factor affecting DLR. COD is generally derived from satellite measurements, however, it should be noted that large uncertainty is still associated with satellite COD retrievals in the regions of elevated and complex terrain. The advantage of the DLR parameterization lies in that it adopt surface meteorological observations as the major inputs. Therefore, it is not common to adopt COD in the DLR parameterizations since COD data are generally not available.

Human cloud observation every 3 or 6 hours are available in meteorological stations before 2013, however, this observation protocol is stopped afterwards. Therefore, human cloud observations are very limited to collocate with our cloud derivations from 1-minute DSR measurements that prevents our attempt to compare cloud cover from human observations and our estimations.

Zhou, Y., Kratz, D. P., Wilber, A. C., Gupta, S. K., & Cess, R. D., An improved algorithm for retrieving surface downwelling longwave radiation from satellite

measurements. J. Geophys. Res., 112(D15), 2007.

Ahn, S. H. , Lee, K. T. , Rim, S. H. , Zo, I. S. , & Kim, B. Y., Surface downward longwave radiation retrieval algorithm for GEO-KOMPSAT-2A/AMI. Asia-Pacific J. Atmos. Sci., 54(2), 237-251, 2018.

Wang, K., and Dickinson, R. E.: Global atmospheric downward longwave radiation at the surface from ground-based observations, satellite retrievals, and re-analyses, Rev. Geophys., 51, 150-185, 10.1002/rog.20009, 2013

Minor comments:

1. The references cited in introduction are pretty outdated. Are there any updated references on such kind of studies?

Reply: we appreciate reviewer's comment here, in the revised version, we update some references in the introduction.

2. Line 185-186: it is better to give an equation on how to calculate DSR.

Reply:

$$DSR_{dir} = 1S_0\tau_r\tau_W\tau_o\tau_a\tau_g$$

where $\tau_r, \tau_w,\ \tau_o,\ \tau_a$ and τ_g are transmittances due to Rayleigh scattering, water vapor absorption, ozone absorption, aerosol extinction and absorption by uniformly mixed gases O_2 and CO_2, respectively. Diffuse radiation is estimated as the sum of the Rayleigh scattered, the aerosol-scattered and the multiple reflected irradiance.

3. Line 189-192: how to deal with aerosol (concentrations, vertical profile, scattering and absorption, etc.) in your calculations? Some details are better provided.

Reply: DSR_{cal} calculation needs the aerosol parameters as follows: Angstrom exponent (α), the Angstrom turbidity (β), single-scattering albedo (ω). For α, and β in NC and AL, the data are from the monthly average of in-situ Cimel photometer measurements. The data in NQ are adopted the same value in AL because both site are at similar high altitude. For ω, we use the average value of 0.90 retrieved from CIE-318 observation in Lhasa (91.13, 29.67, 3663m). Aerosol vertical profile is not considered.

4. Line 193-194: 'The terrain reflection is estimated according to Dozier and Frew (1990)', again please give some descriptions on how to estimate surface albedo.

Reply: We deleted the terrain reflection component since our measurements were made under conditions with no surrounding mountains around sites.

5. Line 197-199: give some description on why use these values as surface albedo, are they from surface measurements?

Reply: Yes, these values are from the surface measurements.

For NQ and AL, the surface albedo value are 0.25 and 0.22, which are derived from the reference (Liang et al., 2012)

Liang H., Zhang R., Liu J., Sun Z., and Cheng X., Estimation of Hourly Solar Radiation at the Surface under Cloudless Conditions on the Tibetan Plateau Using a Simple Radiation Model, Adv. Atmos. Sci., 29(4), 675-689, 2012.

Albedo at NC is 0.183 derived from the reference (Zhao et al., 2011).

Zhao X., Peng B., Qin N., Wang W. (2011), Characteristics of Energy Transfer and Micrometeorology in Surface Layer in Different Areas of Tibetan Plateau in Summer (in Chinese), Plateau and mountain Meteorology Research,31(1), 6-11, 2011.

6. Line 200: why scaled DSR to 1400 W m^{-2}, DSR is net downward shortwave radiation, rather than total solar radiation.

Reply: DSR means downward shortwave radiation, not net downward shortwave radiation. We just adopted 1400 W m^{-2} according to Duchon and O'malley (1998) and Long and Ackerman (2000). It only favors for a clear presentation of the normalized and observation DSR together in the same figure.

7. In addition, the paper would be greatly enhanced with additional proof reading to improve the quality of the written English.

Reply: The manuscript has been extensively revised according to reviewers' comments and suggestions. We tried our best through additional proof readings to eliminate grammar errors.

A revisit of parametrization of downward longwave radiation in summer over the Tibetan Plateau based on high temporal resolution measurements

Mengqi Liu[a,c], Xiangdong Zheng[d], Jinqiang Zhang[a,b,c] and Xiangao Xia[a,b,c]

[a] LAGEO, Institute of Atmospheric Physics, Chinese Academy of Sciences, Beijing, 100029, China

[b] Collaborative Innovation Center on Forecast and Evaluation of Meteorological Disasters, Nanjing University of Information Science & Technology, Nanjing 210044, China

[c] College of Earth and Planetary Sciences, University of Chinese Academy of Sciences, Beijing, 100049, China

[d] Chinese Academy of Meteorological Sciences, Chinese Meteorological Bureau, Beijing, 100081, China

Abstract

The Tibetan Plateau (TP) is one of research hot spots in the climate change research due to its unique geographical location and high altitude. Downward longwave radiation (DLR), as a key component in the surface energy budget, is of practical implications for radiation budget and climate change. A couple of attempts have been made to parametrize DLR over the TP based on hourly or daily measurements and crude clear sky discrimination methods. This study uses 1-minute shortwave and longwave radiation measurements at three stations over TP to parameterize DLR during summer months. Three independent methods are used to discriminate clear sky from clouds based on 1-minute radiation and Lidar measurements. This guarantees strict selection of clear sky samples that is fundamental for the parameterization of clear-sky DLR. Eleven clear-sky and four cloudy DLR parameterizations are examined and locally calibrated. Comparing to previous studies, DLR parameterizations here are shown be characterized by smaller root mean square error (RMSE) and higher coefficient of determination (R^2). Clear-sky DLR can be estimated from the best parametrization with RMSE of 3.8 $W \cdot m^{-2}$ and $R^2 > 0.98$. Systematic overestimation of clear-sky DLR by the locally calibrated parametrization in previous study is found to be approximately 25 $W\ m^{-2}$ (10%), which is very likely due to potential residual cloud contamination on previous clear-sky DLR parametrization. Cloud-base height under overcast conditions is shown to play an important role in cloudy DLR parameterization, which is considered in the locally calibrated parameterization over the TP for the first time. Further studies on DLR parameterization during nighttime and in seasons except summer are required for our better understanding of DLR's role in climate change based on 1-minute high-quality DLR measurements.

1 Introduction

The downward longwave radiation (DLR) at the Earth's surface is the largest component of the surface energy budget, being nearly double the downward shortwave radiation (DSR) (Kiehl and Trenberth, 1997). DLR has shown a remarkable increase during the process of global warming (Stephens et al., 2012). This is closely related to the fact that both a warming and moistening of the atmosphere (especially at the lower atmosphere associated with the water vapor feedback) positively contribute to this change. Understanding of complex spatiotemporal variation of DLR and its implication is necessary for improving weather prediction, climate simulation as well as water cycling modeling. Unfortunately, errors in DLR are considered substantially larger than errors in any of the other components of surface energy balance, which is most likely related to the lack of DLR measurements with high quality (Stephens et al., 2012).

The 2-sigma uncertainty of DLR measurement by using a well-calibrated and maintained pyrgeometer is estimated to be 2.5% or 4 $W \cdot m^{-2}$ (Stoffel, 2005). However, global-wide surface observations are very limited, especially in those remote regions. On the other hand, it has been known for almost one century that clear-sky DLR is determined by the bulk emissivity and effective temperature of the overlying atmosphere (Ångström, 1918). Since these two quantities are not easily observed for a vertical column of the atmosphere, clear-sky DLR is widely parameterized as a function of surface air temperature and water vapor density, assuming that the clear sky radiates toward the surface like a grey body at screen-level temperature. Dozens of parameterization formulas of DLR have been developed in which clear-sky effective emissivity (ε_c) is a function of the screen-level temperature (T) and water vapor pressure (e), or simply in the localized coefficients with given functions. Two formulas, i.e., an exponential function (Idso, 1981) and a power law function (Brunt, 1932; Swinbank, 1963), have been widely used to depict the relationship of ε_c to T and e. The coefficients of these functions are derived by a regression analysis of collocated measurements of T, e and DLR. Most of these proposed parameterizations are empirical in nature and only specific for definite atmospheric condition. An exception is that Brutsaert (1975) developed a model based on the analytic solution of the Schwarzchild's equation for a standard atmospheric lapse rates of T and e. Prata (1996) found that the precipitable water content (w) was much better to represent the effective emissivity of the atmosphere than *e*, which was loosely based on radiative transfer simulations. Dilley and O'Brien (1998) adopted this scheme but tuned empirically their parameterization using an accurate radiative transfer model. Since DLR is to some extent impacted by water vapor and temperature profile (especially in case of existence of an inversion layer) and diurnal variation of *T*, a new model with two more coefficients considering these effects was developed (Dupont et al., 2008a).

In the presence of clouds, total effective emissivity of the sky is remarkably modulated by clouds. The existing clear-sky parameterization should be modified according to the cloud fraction (CF) and other cloud parameters such as cloud base height (CBH). CF is generally used to represent a fairly simple cloud modification under cloudy conditions. Dozens of equations with cloudiness correction have been developed and evaluated by DLR measurements across the world (Crawford and Duchon, 1999; Niemela et al., 2001). CF can be obtained by trained human observers (Iziomon et al., 2003) or derived from DSR (Crawford and Duchon, 1999) and DLR measurements (Durr and Philipona, 2004). High temporal resolution of DSR or DLR measurements (for example, 1-minute) can also provide cloud type information (Duchon and O'Malley, 1999), and thereby allow to consider potential effects of cloud types on DLR (Orsini et al., 2002).

With an average altitude exceeding 4 km above the sea level (ASL), the Tibetan Plateau (TP) exerts a huge influence on regional and global climate through mechanical and thermal forcing because of its highest and most extensive highland in the world (Duan and Wu, 2006). TP, compared to other high altitude regions and the poles, has been relatively more sensitive to climate change. The most rapid warming rate over the TP occurred in the latter half of the 20th century was likely associated with relatively large increase in DLR. Duan and Wu (2006) indicated that increase in low level nocturnal cloud amount and thereby DLR could partly explain the increase in the minimum temperature, despite decrease in total cloud amount during the same period. By using observed sensitivity of DLR to change in specific humidity for the Alps, Rangwala et al. (2009) suggested that increase in water vapor appeared to be partly responsible for the large warming over the TP. Since the coefficients of certain empirical parameterizations and their performances showed spatiotemporal variations, establishment of localized DLR parameterizations over the TP is of highly significance. Further studies on DLR, including its spatiotemporal variability, its parameterization as well as its sensitivity to changes in atmospheric variables, would be expected to improve our understanding of climate change over the TP (Wang and Dickinson, 2013).

DLR measurements from high quality radiometer with high temporal resolution over the TP are quite scarce. To the best of our knowledge, there are very few publications on DLR and its parameterization over the TP. Wang and Liang (2009) evaluated clear-sky DLR parameterizations of Brunt (1932) and Brutsaert (1975) at 36 globally distributed sites, in which DLR data at two TP stations were used. Yang et al. (2012) used hourly DLR data at 6 stations to study major characteristics of DLR and to assess the all-sky parameterization of Crawford and Duchon (1999). Zhu et al. (2017) evaluated 13 clear-sky and 10 all-sky DLR models based on hourly DLR measurements at 5 automatic meteorological stations. The Kipp & Zonen CNR1 is composed of CM3 pyranometer and CG3 pyrgeometer that are used to measure DLR and DSR, respectively. The CG3 is the second class radiometer according to the International Organization for Standardization (ISO) classification. The root mean square of hourly DLR is less than 5 Wm^{-2} after field recalibration and window heating correction (Michel et al., 2008). Note that human observations of cloud every 3-6 hours or hourly DLR and DSR data are respectively used to determine clear sky and cloud cover in these previous studies.

In order to further our understanding of DLR and DSR over the TP, measurements of 1-minute DSR and DLR at 3 stations over the TP using state-of-the-art instruments have been performed in summer months since 2011. These data provide us opportunity to evaluate clear-sky DLR models and quantitatively assess cloud impacts on DLR. This study makes progress in the following aspects as compared to previous studies: 1) clear-sky discrimination and CF estimation are based on 1-minute DSR and DLR measurements that are objective in nature; 2) misclassification of cloudiness into cloud-free skies would be minimized by adopting strict cloud-screening procedures based on 1-minute DSR, DLR and Lidar measurements; 3) potential effects of CBH on DLR are also investigated. Localized parameterizations of clear-sky and all-sky DLRs are finally achieved, which would be expected to improve DLR estimations over the TP.

2. Site, Instrument and Data

Measurements of DLR and DSR are conducted 1~4 months over the TP at three stations (Table 1), including Nagqu (NQ, 92.04°E, 31.29°N, 4507 m ASL), Nyingchi (NC, 94.2°E, 29.4°N, 2290 m ASL) and Ali (AL, 80°E, 32.5°N, 4287 m ASL). DLR and DSR were respectively measured by CG4 and CM21 radiometers (Kipp & Zonen, Delft, Netherlands). The sampling frequency is 1 Hz and the averages of the samples over 1-minute intervals are logged on a Campbell Scientific CR23X datalogger. Simultaneous 1-minute averages of T and e are taken from the automatic meteorological stations. With the aid of its specific material and unique construction, CG4 is designed for the DLR measurement with high reliability and accuracy. Window heating due to absorption of solar radiation in the window material, the major error source of DLR measurement, is strongly suppressed by its unique construction conducting away the absorbed heat very effectively. CM21 is a high performance research grade pyranometer. Introduction of individually optimized temperature compensation for CM21 makes it having much a smaller thermal offset than CM3. The installation of the CG4 and CM21 on the Kipp & Zonen CV2 ventilation unit prevents dew deposition on the window of the CG4 and the quartz dome of the CM21. The radiometers are calibrated before and after field measurements to the standards held by the China National Centre for Meteorological Metrology.

A Micropulse Lidar (MPL-4B, Sigma Space Corporation, United States) was installed site-by-site with radiometers. The Nd:YLF laser of the MPL produces an output power of 12 μJ at 532 nm. The repletion rate is 2500 Hz. The vertical resolution of the MPL data is 30 m and the integration time of the measurements is 30s. The MPL backscattering profiles are used to identify the cloud boundaries and derive the CBHs (He et al., 2013). The dataset contains about 700 hours of coincident DLR, DSR, Lidar and meteorological measurements.

3. Methods

3.1 Clear-sky discrimination

Clear skies should be discriminated from cloudy conditions before performing DLR parametrization, which is achieved by the synthetical analysis of DSR, DLR, and CBH from MPL.

Following the method initiated by Crawford and Duchon (1999), we calculate two quantities reflecting DSR magnitude and variability based on 1-minute observed DSR (DSR_{obs}) and calculated clear-sky DSR (DSR_{cal}) values. DSR_{cal} is calculated by the model C of Iqbal (1983), in which direct and diffuse DSR are parametrized separately. Direct DSR ($\mathrm{DSR_{dir}}$) is calculated as follows.

$$DSR_{dir} = S_0 \tau_r \tau_W \tau_o \tau_a \tau_g \qquad (1)$$

where τ_r, τ_w, τ_o, τ_a and τ_g are transmittances due to Rayleigh scattering, water vapor absorption, ozone absorption, aerosol extinction and absorption by uniformly mixed gases O_2 and CO_2, respectively; S_0 is eccentricity-corrected extraterrestrial solar radiation. Diffuse radiation is estimated as the sum of Rayleigh and aerosol scattering as well as multiple reflectance. Total ozone column (DU) is provided by Brewer spectrophotometer. *w* values (cm) are from Vaisala-92 radiosonde profiles in AL and Global Position System measurements in NC and NQ, respectively. They are used to create linear regression relationship to collocated ground level *e* (hPa) measurements, which is then used to estimate *w* from 1-minute measurements of *e*. Ångström wavelength exponent and Ångström turbidity are from CIE-318 sunphotometer observations in NC and AL, while in NQ we adopt the same value as that in AL. Mean single scattering albedo retrieved from CIE-318 observation in Lhasa (91.13, 29.67, 3663m) is 0.90 (Che et al., 2019), which is used in three stations. Surface Albedo is 0.25 and 0.22 in Al and NQ according to in situ measurements (Liang et al., 2012). In NC, it is 0.183 (Zhao et al., 2011).

DSR_{cal} values are first scaled to a constant value of 1400 $W{\cdot}m^{-2}$ for each minute of each day. We adopt this value according to Duchon and O'malley (1998) and Long and Ackerman (2000), which only favors for a clear presentation of the normalized and observed DSR values in the same figure. Afterwards, DSR_{obs} values are scaled by multiplying the same set of scale factors. Finally, the mean and standard deviation of the scaled DSR in a 21-minute moving window (±10 minute centered on the time of interest) are used for cloud screening. Selection of the width of 21-minute is empirical but a consequence of having a reasonable time span for estimating the mean and variance (Duchon and O'Malley, 1999). Clear-sky DSR should satisfy three requirements: 1) ratio of DSR_{obs} to DSR_{cal} is within 0.95 to 1.05; 2) difference between scaled DSR_{obs} and DSR_{cal} is less than 20 $W{\cdot}m^{-2}$; and 3) standard deviation (δ) of scaled DSR_{obs} in a 21-minute moving window is less than 20 $W{\cdot}m^{-2}$.

Temporal variability of DLR is also used for cloud screening according to Marty and Philipona (2000) and Sutter et al. (2004). Here, δ of scaled DLR (scaled to 500 W·m^{-2}) in a 21-minute moving window is used for this purpose. Cloud-free sample is determined if δ is less than 5 W·m^{-2}.

Since both DSR and DLR experience difficulties in detecting clouds in the portion of the sky far away from the sun (Duchon and O'Malley, 1999) or high-altitude cirrus clouds (Dupont et al., 2008b), coincident MPL backscatter measurements are used to strictly select clear-sky samples. There should be a cloud element somewhere in the sky when MPL identifies cloud, it is thus required that no clouds are detected by MPL in a 21-minute moving window, otherwise it is defined as cloudy.

Given the fact that these methods are complementary to each other to some extent (Orsini et al., 2002), we use the following strategy to guarantee a proper selection of clear-sky samples. If DSR, DLR and MPL measurements at the time of interest synchronously satisfy these specified clear-sky conditions, the sample is thought to be taken under unambiguously cloud-free condition; on the contrary, the measurement are made under unambiguously cloudy condition if any method suggests cloudy. Our following clear-sky and cloudy DLR parameterizations are respectively based on measurements under unambiguously cloud-free (8195 minutes) and cloudy conditions (69318 minutes).

Fig. 1 shows an example of clear sky discrimination results based on our method. DSR_{obs} presents a smooth temporal variation from sunrise to about 14:00 (LST), being consistent with DSR_{clr}. Similarly, DLR also varies very smoothly during the same period when 21-minute standard deviations of DLR are < 5 W·m^{-2}. Both facts suggest sunny and cloudless skies. This inference is supported by MPL that suggests no cloud detected overhead. Contrarily, an abruptly changes of 1-minute DSR_{obs} and DLR are evident during 14:00~17:00 LST and we can see DSR_{obs} occasionally exceeds the expected DSR_{clr}, indicating frequent occurrence of fair weather cumuli clouds. MPL detect a persistent thin cloud layer at 4 km above ground, which agrees with DSR and DLR measurements very well.

3.2 Cloud fraction estimation

Given synoptic cloud observations are very limited and temporally sparse, various parameterizations using DSR or DLR data have been developed to estimate CF (e.g., Deardorff, 1978; Marty and Philipona, 2000; Durr and Philipona, 2004; Long et al., 2006; Long and Turner, 2008). Because of good agreement between clear-sky DSR_{obs} and DSR_{cal} calculated by the Iqbal model C (Iqbal, 1983; Gubler et al., 2012), with mean bias of 1.7 $W \cdot m^{-2}$ and root mean square error (RMSE) of 10.7 $W \cdot m^{-2}$ (not shown), we use Deardorff (1978)'s method to calculate CF from DSR_{obs} and DSR_{cal}. The method is based on a fairly simple cloud modification to DSR as follows.

$$\mathrm{CF} = 1 - \frac{\mathrm{DSR}_{obs}}{\mathrm{DSR}_{cal}} \quad (2)$$

CF (no unit) has values ranging from 0 to 1. To avoid the error caused by abrupt DSR variation, 21-minute mean DSR value rather than its instantaneous measurements are used here.

4 Results

4.1 Clear-sky DLR parameterization evaluation and localization

Eleven clear-sky DLR (DLR_{clr}) parameterizations (Table 2) are evaluated based on 1-minute DLR measurements under unambiguously cloud-free conditions. To compare the performance of these 11 models, RMSE and the coefficient of determination (R^2) are shown by a Taylor diagram in Fig. 2(a). Relatively smaller RMSE (generally < 15 $W \cdot m^{-2}$) and larger R^2 (>0.95) are derived for the Brutsaert (1975); Konzelmann (1994), Dilley and O'Brien (1998) and Prata (1996) models. This is likely because these parameterizations were developed in cool and dry areas, for example, in England (Brutsaert, 1975); in Greenland (Konzelmann, 1994) and dry desert region in Australia (Prata, 1996). The climate in those areas is likely similar to that over the TP to some extent, so those parameterizations are expected to perform well. The higher RMSE (>37 $W \cdot m^{-2}$) and the lower R^2 (~0.7) are derived for Swinbank (1963) and Idso and Jackson (1969) models. This can be partly explained by the fact that only T is used in these two methods. Previous studies suggests substantial uncertainty (RMSE >37.5 $W \cdot m^{-2}$ and R^2 <0.75) if water vapor effect on DLR_{clr} is not accounted for (Duarte et al., 2006). Since w is very low over the TP and thereby DLR is highly sensitive to variation of w in that case, much more attention should be paid to water vapor effect on the parameterization of DLR_{clr}.

The coefficients in eleven parameterizations (Table 2) were originally calibrated and determined in different geographical locations; therefore, they may not be the optimal values for the TP. Thus we take use of 1-minute clear-sky DLR samples to locally calibrate the parameters of these parametrizations. We use 10-fold cross-validation method to determine the parameters. This is a widely used method to estimate the skill of a regression model on unseen data. It is expected to result in a less biased or less optimistic estimate of the model skill than other methods, such as a simple train/test split (James et al., 2013). All the data was randomly dividing into 10 groups of approximately equal size, the coefficients are computed by using 9 groups as training set, and the remaining 1 group is used as validation. This procedure is repeated 10 times to get the representational value of coefficients (with the lowest test error).

The coefficient values derived from the non-linear least-squares fitting of the DLR_{clr} parameterizations (Table 2) over the TP are presented in Table 3. For each fitted parameterization, we calculated RMSE and R^2 and the results are shown in Fig. 2b. When using the parameterizations with the locally fitted parameters, the accuracy of the parameterization relative to the published values is obviously improved. Most RMSEs are < 10 $W \cdot m^{-2}$ except the parameterization proposed by Swinbank (1963) and Idso and Jackson (1969) that still produce the worst results (with R^2 of 0.71 and RMSE of 15 $W \cdot m^{-2}$) even after the parameters are locally calibrated.

The Dilley and O'Brien (1998)'s parameterization, which is initially developed by considering the adaptation of climatological diversities, is expected to be able to fit the measurements in tropical, mid-latitude and Polar Regions. This expectation is verified by its wide deployment in DLR_{clr} estimations in different climate regimes and altitude levels, for example, in the tropical lowland (eastern Pará state, Brazil) and the mild mountain area (Boulder, the United States) (Marthews et al., 2012; Li et al., 2017). The present study confirms that Dilley and O'Brien (1998) is the best clear-sky parameterization over the TP. The locally calibrated equation is as follows.

$$\mathrm{DLR}_{clr} = -2.53 + 158.10 \times \left(\frac{T}{273.16}\right)^6 + 106.40 \times \left(\frac{46.50 \times \frac{e}{T}}{2.50}\right)^{\frac{1}{2}} \qquad (3)$$

Where T and e represent air temperature (K) and water vapor pressure (hPa), respectively (T and e have the same meaning and unit in following equations if not specified). The RMSE and R^2 of Eq.(3) are ~3.8 $W \cdot m^{-2}$ and > 0.98 respectively, which are substantially lower than those in previous studies over the TP, for example, the RMSE was

9.5 W·m^{-2} (Zhu et al., 2017). The Dilley and O'Brien (1998)'s parameterization was suggested to be the most reliable estimates of DLR_{clr} over the TP (Zhu et al., 2017). Note that the parameters here differ quite a lot from their values (Zhu et al., 2017), as shown in Eq. (4).

$$\mathrm{DLR}_{clr}=30.00+157.00\times\left(\frac{T}{273.16}\right)^{6}+97.93\times\left(\frac{46.50\times\frac{e}{T}}{2.50}\right)^{\frac{1}{2}} \quad (4)$$

Fig.3 compares instantaneous clear-sky DLR data from measurements against calculations by Eq. (3) of this study and by Eq. (4) from Zhu et al. (2017). The former performs very well as shown by an overwhelmingly large number of data points falling along or overlapping the 1:1 line. By contrast, the latter overestimates DLR by 25 W·m^{-2} (10%). This difference is not very likely due to different DLR measurements used to produce Eq. (3) and (4) giving the following considerations. First, this systematic overestimation is much larger than the expected uncertainty of DLR measurements (2.5% or 4 W·m^{-2}) (Stoffel, 2005). More important, comparison of cloudy DLR parameterizations between this study and Zhu et al. (2017) showed good agreement (not shown). Note that only 1-hour CG3 DLR observations are used for clear sky discrimination in Zhu et al. (2017). This method was shown to be very likely contaminated by the thin high cloud (Sutter et al., 2004). This certainly would produce an overestimation of clear sky DLR parameterization since larger DLRs are associated with potential residual clouds relative to real clear sky DLRs.

4.2 Parameterization of cloudy-sky DLR

Parameterizations of cloudy-sky DLR (DLR_{cld}) are based on estimated DLR_{clr} coupled with the effect of cloudiness or cloud emissivity, which depends primarily on CF as well as other cloud parameters, like CBH and cloud type (Arking, 1990; Viúdez-Mora et al., 2015). Four parameterizations (Table 4), which modifies the bulk emissivity depending on CF, are assessed and locally calibrated in this section.

DLR_{clr} is estimated according to Eq. (3). The fitted values of the coefficients (using 10-Fold Cross-Validation) of the four cloudy parameterizations are presented in Table 5. RMSE and R^2 of original and locally fitted parameterizations over the TP are presented in Fig. 4.

Relative to clear-sky conditions, cloudy parameterizations using the given parameters have higher error RMSE (generally exceeding 35 W·m^{-2}) except that developed by Jacobs

(1978) (RMSE of 18 W·m^{-2}). R^2 was generally smaller than 0.9. RMSE values decrease significantly in Maykut and Church (1973) and Sugita and Brutsaert (1993) as locally calibrated parameters are used. Relative smaller and almost no RMSE improvements are found for the methods developed by Konzelmann (1994) and Jacobs (1978).

Eq. (5) shows the best cloudy-sky parameterization over the TP by combining the clear-sky parameterization of Dilley and O'Brien (1998) with the cloud modulation correction scheme of Jacobs (1978).

$$\mathrm{DLR}_{cld} = (1 + 0.23 \times \mathrm{CF}) \times \left(59.38 + 113.70 \times \left(\frac{T}{273.16}\right)^6 + 96.96 \times \left(\frac{46.50 \times \frac{e}{T}}{2.50}\right)^{\frac{1}{2}}\right) \qquad (5)$$

RMSE and R^2 are ~18 W·m^{-2} and ~0.89 respectively. RMSE here is close to 15 W·m^{-2} obtained in different altitude areas in Swiss (Gubler et al., 2012) and slightly lower than 23 W·m^{-2} obtained in mountain area in Germany (Iziomon et al., 2003). Comparing to previous studies over the TP (RMSE of 22 W m^{-2} in Zhu et al., 2017), our cloudy model produces better results.

4.3 Effect of CBH on DLR under Overcast Conditions

Since clouds behave approximately as a blackbody, the most relevant cloud parameter (besides CF) to DLR under overcast skies (DLR_{ovc}) is the temperature of its lower boundary (CBH). Radiative transfer model simulation has suggested that CBH under overcast conditions is an important modulator for DLR. The cloud radiation effect (CRE), the difference between DLR_{obs} and DLR_{clr}, decreases with increasing CBH at a rate of 4~12 W·m^{-2} that depends on climate profiles (Viúdez-Mora et al., 2015). This indicates that cloudy DLR parameterization would be improved if CBH is considered.

The statistical relationship between CRE and CBH under overcast conditions over the TP is presented in Fig. 5. The peak and median values of CRE decrease with the increase of CBH from the box plot in Fig.5. CRE variation increases from 25 to 50 W·m^{-2} as CBH increases because water vapor influence and its variation goes up. Compared to Viúdez-Mora (2015) results derived at Girona, Spain, a mid-latitude site with low altitude, CRE over the TP is generally lower by 5~10 W·m^{-2}. This is likely because clouds over the TP with the same CBH as that at Girona have relatively lower temperature, thereby producing lower radiative effect on DLR. It is interesting that the decreasing tendency of CRE with

CBH is apparent. CRE is about 70 W·m^{-2} for clouds < 1 km and decreases to ~40 W·m^{-2} for clouds at 3~4 km in TP. The decreasing rate of CRE with CBH is estimated to be -9.8 W·m^{-2}·km^{-1} over the TP that agrees with model simulations (Viúdez-Mora et al., 2015).

To consider CBH effect under overcast conditions, we introduced a modified parameterization according to Viúdez-Mora et al. (2015):

$$\mathrm{DLR}_{ovc} = 1.23 \times \mathrm{DLR}_{clr} \times (1.01 - 0.06 \times \mathrm{CBH}) \quad (6)$$

Where CBH has unit of km. The bias and RMSE of Eq. (6) between measurements and calculations is 1.3 W·m^{-2} and 16.5 W·m^{-2}, respectively, which are significantly lower than that of Eq. (5) (10.3 W·m^{-2} and 21.4 W·m^{-2}) in overcast conditions. The result indicates a remarkable improvement in the estimation of DLR under overcast conditions by introducing CBH to the DLR parameterization.

5 Discussion and conclusions

The parameterization of clear-sky DLR requires a well-defined distinction between clear-sky and cloudy-sky situations that commonly depends on human cloud observations 4~6 times each day. Human observation is subjective in nature and its low temporal resolution cannot resolve dramatic high-resolution variation of clouds. Furthermore, synoptic human cloud observations show the tendency to stronger weight to the horizon that DLR is not highly sensitive (Marty and Philipona, 2004). Clear sky discrimination based on hourly DSR or DLR measurements also tends to be very suspect of residual clouds due to their low temporal resolution. Parameterization of clear-sky DLR based on these two methods is hence very likely biased as a consequence of selection of cloud contaminated clear-sky measurements. This would result in biased estimation of cloud DLR effect since it is the difference between clear-sky and measured all-sky DLRs (Dupont et al., 2008b).

Using 1-minute DSR and DLR at 3 stations over the TP, DLR parameterizations are evaluated and localized parameterizations have been developed based on a comprehensive cloud-screening method. Potential CBH effect on overcast DLR is experimentally determined. Major conclusions are as follows.

Among 11 clear-sky DLR parameterizations tested in this study, two methods using only atmospheric temperature largely deviate from other parameterizations. The best method suitable for TP is the parameterization developed by Dilley and O'Brien (1998). DLR estimation can be improved by localization of these parameterizations. Locally calibrated parameterization can produce clear sky DLR with RMSE of 3.8 W·m^{-2}.

Overcast DLR is highly sensitive to CBH. The parameterization can be substantially improved by consideration of CBH effect. The bias between empirically parameterized calculations and measurements decreases from 10.3 to 1.3 W·m^{-2}.

The focus of this study is on daytime DLR parameterization over the TP since DSR is used in the cloud-screening method. Given a significant role of DLR played in the surface energy budget during nighttime, it is highly desirable to perform further study on the nighttime DLR parametrization. These results are based on summer DLR measurements, so the conclusions here need to be further tested in other seasons, especially in winter when an increasing tendency of DLR has been observed (Rangwala et al., 2009). Further investigations on these issues are expected to shed new light on how and why DLR has changed over the TP.

Acknowledgements: This work was supported by the Strategic Priority Research Program of Chinese Academy of Sciences (XDA17010101), the National Key R&D Program of China (2017YFA0603504), the National Natural Science Foundation of China (91537213 and91637107), the Special Fund for Meteorological Research in the Public Interest (GYHY201106023), and the Science and Technological Innovation Team Project of Chinese Academy of Meteorological Science (2013Z005) respectively support the observations at AL, NQ and NC. We greatly appreciate Dr. Q. He for providing the MPL Lidar measurement images and derived CBH data.

References

Ångström, A.: A study of the radiation of the atmosphere, Smithsonian Miscellaneous Collection, 65, 1–159, 1915.

Arking, A.: The radiative effects of clouds and their impact on climate, Bull. Am. Meteorol. Soc., 72, 795-813, 10.1175/1520-0477(1991)072<0795:Treoca>2.0.Co;2, 1991.

Brunt, D.: Notes on radiation in the atmosphere, Q. J. Roy. Meteorol. Soc., 58, 389–420, 1932.

Brutsaert, W.: On a derivable formula for long-wave radiation from clear skies, Water Resource Res., 11, 742–744, 1975.

Carmona, F., Rivas, R., and Caselles, V.: Estimation of daytime downward longwave radiation under clear and cloudy skies conditions over a sub-humid region, Theor. Appl. Climatol., 115, 281-295, 10.1007/s00704-013-0891-3, 2014.

Che, H., Xia, X., Zhao, H., Dubovik, O., Holben, B. N., Goloub, P., Cuevas-Agulló, E., Estelles, V., Wang, Y., Zhu, J., Qi, B., Gong, W., Yang, H., Zhang, R., Yang, L., Chen, J., Wang, H., Zheng, Y., Gui, K., Zhang, X., and Zhang, X.: Spatial distribution of aerosol microphysical and optical properties and direct radiative effect from the China Aerosol Remote Sensing Network, Atmos. Chem. Phys. Discuss., https://doi.org/10.5194/acp-2019-405, in review, 2019.

Crawford, T. M., and Duchon, C. E.: An improved parameterization for estimating effective atmospheric emissivity for use in calculating daytime downwelling longwave radiation, J. Appl. Meteorol., 38, 474–480, 1998.

Deardorff, J. W.: Efficient prediction of ground surface temperature and moisture, with an inclusion of a layer of vegetation. J. Geophys. Res., 83, 1889–1903, 1978.

Dilley, A. C., and O'Brien, D. M.: Estimating downward clear sky long-wave irradiance at the surface from screen temperature and precipitable water, Q. J. Roy. Meteorol. Soc., 124a, 1391–1401, 1997.

Dozier, J., and Frew, J.: Rapid calculation of terrain parameters for radiation modeling from digital elevation data, IEEE T. Geosci. Remote, 28, 963–969, 1990.

Dominik, M., R. Philipona, C. Ruckstuhl, R. Vogt and L. Vuileumier, Performance and uncertainty of CNR1 net radiometers during a one-year field comparison, J of Atmos., and Ocean. Tech., 25(3), 442-451, 2008.

Duan, A., and Wu, G.: Change of cloud amount and the climate warming on the Tibetan Plateau, Geophys. Res. Lett., 33, 10.1029/2006gl027946, 2006.

Duarte, H. F., Dias, N. L., and Maggiotto, S. R.: Assessing daytime downward longwave radiation estimates for clear and cloudy skies in Southern Brazil, Agr. Forest. Meteorol., 139, 171-181, 10.1016/j.agrformet.2006.06.008, 2006.

Duchon, C. E., and O'Malley, M. S.: Estimating cloud type from pyranometer observations, J. Appl. Meteorol., 38, 132-141, 1999.

Dupont, J. C., Haeffelin, M., Drobinski, P., and Besnard, T.: Parametric model to estimate clear-sky longwave irradiance at the surface on the basis of vertical distribution of humidity and temperature, J. Geophys. Res., 113, 10.1029/2007jd009046, 2008.

Durr, B., and Philipona, R.: Automatic cloud amount detection by surface longwave downward radiation measurements, J. Geophys. Res., 109, 9, 10.1029/2003jd004182, 2004.

Gubler, S., Gruber, S., and Purves, R. S.: Uncertainties of parameterized surface downward clear-sky shortwave and all-sky longwave radiation, Atmos. Chem. Phys., 12, 5077-5098, 10.5194/acp-12-5077-2012, 2012.

He, Q. S., Li, C. C., Ma, J. Z., Wang, H. Q., Shi, G. M., Liang, Z. R., Luan, Q., Geng, F. H., and Zhou, X. W.: The properties and formation of cirrus clouds over the Tibetan Plateau based on summertime lidar measurements, J. Atmos. Sci., 70, 901-915, 10.1175/jas-d-12-0171.1, 2013.

Idso, S. B.: A set of equations for full spectrum and 8 to 14 μm and 10.5 to 12.5 μm thermal radiation from cloudless skies, Water Resource Res., 17, 295–304, 1981.

Iqbal, M.: An Introduction to Solar Radiation, Academic Press, Toronto, Canada, 1983.

Iziomon, M. G., Mayer, H., and Matzarakis, A.: Downward atmospheric longwave irradiance under clear and cloudy skies: measurement and parameterization, J. Atmos. Solar-Terr. Phys., 65, 1107–1116, 2003.

Jacobs, J.D.: Radiation climate of Broughton Island, in: Energy Budget Studies in Relation to Fast-ice Breakup Processes in Davis Strait, edited by Barry, R. G. and Jacobs, J. D., Inst. of Arctic and Alp. Res. Occas. Paper No. 26. University of Colorado, Boulder, pp. 105–120, 1978.

James, G., Witten, D., Hastie, T., and Tibshirani, R.: An Introduction to Statistical Learning:

with Applications in R, Springer-Verlag New York, USA, 2013.

Kiehl, J. T., and Trenberth, K. E.: Earth's annual global mean energy budget. Bull. Am. Meteorol. Soc., 78, 197-208, 1997.

Konzelmann, T., van de Wal, R. S. W., Greuell, W., Bintanja, R., Henneken, E. A. C., and Abe-Ouchi, A.: Parameterization of global and longwave incoming radiation for the Greenland Ice Sheet, Global Planet. Change, 9, 143–164, 1994.

Kruk, N. S., Vendrame, I. F., da Rocha, H. R., Chou, S. C., and Cabral, O.: Downward longwave radiation estimates for clear and all-sky conditions in the Sertozinho region of So Paulo, Brazil, Theor. Appl. Climatol., 99, 115-123, 2010.

Li, M. Y., Jiang, Y. J., and Coimbra, C. F. M.: On the determination of atmospheric longwave irradiance under all-sky conditions, Sol. Energy., 144, 40-48, 10.1016/j.solener.2017.01.006, 2017.

Liang, H., Zhang, R. H., Liu, J. M., Sun, Z. A., and Cheng, X. H.: Estimation of hourly solar radiation at the surface under cloudless conditions on the Tibetan Plateau using a simple radiation model, Adv. Atmos. Sci., 29, 675-689, 10.1007/s00376-012-1157-1, 2012.

Long, C. N., Ackerman, T. P., Gaustad, K. L., and Cole, J. N. S.: Estimation of fractional sky cover from broadband shortwave radiometer measurements, J. Geophys. Res., 111, 11, 10.1029/2005jd006475, 2006.

Long, C. N., and Turner, D. D.: A method for continuous estimation of clear-sky downwelling longwave radiative flux developed using ARM surface measurements, J. Geophys. Res., 113, 16, 10.1029/2008jd009936, 2008.

Marthews, T. R., Malhi, Y., and Iwata, H.: Calculating downward longwave radiation under clear and cloudy conditions over a tropical lowland forest site: an evaluation of model schemes for hourly data, Theor. Appl. Climatol., 107, 461-477, 10.1007/s00704-011-0486-9, 2012.

Marty, C., and Philipona, R.: The Clear-Sky Index to separate clear-sky from cloudy-sky situations in climate research, Geophys. Res. Lett., 27, 2649-2652, 10.1029/2000gl011743, 2000.

Maykut, G. A., and Church P. E.: Radiation climate of Barrow, Alaska, 1962–1966, J. Appl. Meteorol., 12, 620–628, 1973.

Niemelä, S., Räisänen, P., and Savijärvi, H.: Comparison of surface radiative flux parameterizations: Part I: Longwave radiation, Atmos. Res., 58, 1–18, 2001a.

Orsini, A., Tomasi, C., Calzolari, F., Nardino, M., Cacciari, A., and Georgiadis, T.: Cloud cover classification through simultaneous ground-based measurements of solar and infrared radiation, Atmos. Res., 61, 251-275, 10.1016/s0169-8095(02)00003-0, 2002.

Prata, A. J.: A new long-wave formula for estimating downward clear-sky radiation at the surface, Q. J. Roy. Meteorol. Soc., 122, 1127–1151, 1996.

Rangwala, I., Miller, J. R., and Xu, M.: Warming in the tibetan plateau: possible influences of the changes in surface water vapor. Geophys. Res. Lett., 36, 295-311, 2009.

Satterlund, D. R.: An improved equation for estimating longwave radiation from the atmosphere, Water Resource Res., 15, 1649–1650, 1979.

Stephens, G. L., Wild, M., Stackhouse, P. W., Jr., L'Ecuyer, T., Kato, S., and Henderson, D. S.: The global character of the flux of downward longwave radiation, J. Climate., 25, 2329-2340, 10.1175/jcli-d-11-00262.1, 2012.

Stoffel, T.: Solar infrared radiation station (SIRS) handbook, Tech. Rep., ARM TR-025, Atmos. Radiat. Measure. Program, U.S. Dep. of Energy, Washington, D.C, 2005.

Sugita, M., and Brutsaert, W.: Cloud effect in the estimation of instantaneous downward longwave radiation, Water Resource Res., 29, 599-605, 10.1029/92wr02352, 1993.

Swinbank, W. C.: Long-wave radiation from clear skies, Q. J. Roy. Meteo. Soc., 89, 330–348, 1963.

Viúdez-Mora, A., Costa-Surós, M., Calbó, J., and González, J. A.: Modeling atmospheric longwave radiation at the surface during overcast skies: The role of cloud base height, J. Geophys. Res. Atmos., 120, 199–214, 10.1002/ 2014JD022310, 2015.

Wang, K., and Liang, S.: Global atmospheric downward longwave radiation over land surface under all-sky conditions from 1973 to 2008, J. Geophys. Res., 114, 10.1029/2009jd011800, 2009.

Wang, K., and Dickinson, R. E.: Global atmospheric downward longwave radiation at the surface from ground-based observations, satellite retrievals, and reanalyses, Reviews of Geophysics, 51, 150-185, 10.1002/rog.20009, 2013.

Yang, K., Ding, B., Qin, J., Tang, W., Lu, N., and Lin, C.: Can aerosol loading explain the solar dimming over the Tibetan Plateau? Geophys. Res. Lett., 39, 10.1029/2012gl053733, 2012.

Zhao X., Peng B., Qin N., Wang W. (2011), Characteristics of Energy Transfer and Micrometeorology in Surface Layer in Different Areas of Tibetan Plateau in Summer (in Chinese), Plateau and mountain Meteorology Research,31(1), 6-11, 2011.

Zhu, M. L., Yao, T. D., Yang, W., Xu, B. Q., and Wang, X. J.: Evaluation of parameterizations of incoming longwave radiation in the high-mountain region of the Tibetan Plateau, J. Appl. Meteorol. Climatol., 56, 833-848, 10.1175/jamc-d-16-0189.1, 2017.

Table 1: Description of stations and measurements (magnitude and variability) in the Tibetan Plateau

Site	Altitude (m ASL)	Period	T (°C)	e (hPa)	DLR ($W \cdot m^{-2}$)	Data Points
NQ	4507	2011.7.20-2011.8.26	9.4±8	7.4±5	242.75±40	52980
NC	2290	2014.6.7-2014.7.31	16.8±10	13.4±4	368.25±40	69609
AL	4279	2016.5.27-2016.9.22	7.8±4	4.8±4	253.11±50	86596

Table 2. 11 clear-sky DLR parameterizations and their specific conditions

Reference	Clear-Sky Parameterization	Conditions
Angstrom (1915)	$\mathrm{DLR}_{clr} = \{0.83 - 0.18 \times 10^{-0.067e})\}\sigma T^4$	Alt.: 1650~3500 T: 283.15~303.15 e: 4~1
Brunt (1932)	$\mathrm{DLR}_{clr} = (0.52 + 0.065\sqrt{e})\sigma T^4$	Alt.: 6~3500 T: 269.15~303.15 e: 2.5~16
Swinbank (1963)	$\mathrm{DLR}_{clr} = 5.31 \times 10^{-13} T^6$	Alt: 2 T: 281.15~302.15 e: 8~30
Idso and Jackson (1969)	$\mathrm{DLR}_{clr} = (1 - 0.261 \cdot \exp(-0.000777 \times (273 - \mathrm{T})^2))\sigma T^4$	Alt.: 3, 331 T: 228.15~318.15
Brutsaert (1975)	$\mathrm{DLR}_{clr} = 1.24 \left(\frac{e}{T}\right)^{\frac{1}{7}} \sigma T^4$	Alt.: 6~3500 T: 269.15~313.15 e: 2.5~-16
Satterlund (1979)	$\mathrm{DLR}_{clr} = 1.08 \left(1 - \exp\left(-e^{\frac{T}{2016}}\right)\right)\sigma T^4$	Alt.: 594 T: 236.15~309.15 e: 0~18hPa
Idso (1981)	$\mathrm{DLR}_{clr} = \left(0.7 + 5.95 \times 10^{-5} \times e \times \exp\left(\frac{1500}{T}\right)\right)\sigma T^4$	Alt.: 331 T: 258.15~278.15 e: 2~6
Konzelmann (1994)	$\mathrm{DLR}_{clr} = \left(0.23 + 0.443 \left(\frac{e}{T}\right)^{\frac{1}{8}}\right)\sigma T^4$	Alt.: 340~3230 T: 257.15~279.15 e: 1.5~5.5
Prata (1996)	DLR_{clr}=(1-(1+46.5$\frac{e}{T}$) ×exp(-(1.2+3×46.5 $\frac{e}{T}$)$^{0.5}$)) σT^4	Not specified
Dilley and O'Brien (1998)	DLR_{clr}=59.38+113.7$\left(\frac{T}{273.16}\right)^6$ + 96.96$\sqrt{46.5\frac{e}{T}/2.5}$	Not specified
Iziomon (2001)	$\mathrm{DLR}_{clr} = \left(1 - 0.43 \exp\left(-\frac{11.5e}{T}\right)\right)\sigma T^4$	Alt.: 1489 $\bar{T}$=277.55$\bar{e}$ =7.4

*Where Alt. is the altitude above sea level, and its unit is (m ASL), e is screen-level water vapor pressure in hPa and T represents surface temperature in K

Table 3. Locally fitted clear-sky DLR parameterizations in TP

Reference	Locally fitted Clear-Sky Parameterization
Angstrom(1915)	$\mathrm{DLR}_{clr} = \{0.8 - 0.19 \times 10^{-0.068e})\}\sigma T^4$
Brunt(1932)	$\mathrm{DLR}_{clr} = (0.56 + 0.07\sqrt{e})\sigma T^4$

Swinbank(1963)	$\mathrm{DLR}_{clr} = 4.7 \times 10^{-13} T^6$
Idso & Jackson(1969)	$\mathrm{DLR}_{clr} = (1 - 0.36 \cdot \exp(-0.00065 \times (273 - T)^2))\sigma T^4$
Brutsaert(1975)	$\mathrm{DLR}_{clr} = 1.03 \left(\frac{e}{T}\right)^{0.09} \sigma T^4$
Satterlun (1979)	$\mathrm{DLR}_{clr} = \left(1 - \exp\left(-e^{\frac{T}{2016}}\right)\right)\sigma T^4$
Idso(1981)	$\mathrm{DLR}_{clr} = \left(0.63 + 7.5 \times 10^{-5} \times e \times \exp\left(\frac{1500}{T}\right)\right)\sigma T^4$
Konzelmann(1994)	$\mathrm{DLR}_{clr} = \left(0.23 + 0.45\left(\frac{e}{T}\right)^{0.13}\right)\sigma T^4$
Prata(1996)	DLR_{clr}=(1-(1+46.5$\frac{e}{T}$) ×exp(-(1+3×46.5$\frac{e}{T}$)$^{0.5}$)) σT^4
Dilley and O'Brien(1998)	DLR_{clr}=-2.54+158.1$\left(\frac{T}{273.16}\right)^6 + 106.4\sqrt{46.5\frac{e}{T}/2.5}$
Iziomon(2001)	$\mathrm{DLR}_{clr} = \left(1 - 0.38\exp\left(-\frac{14.52e}{T}\right)\right)\sigma T^4$

Table 4. 4 Cloudy-sky DLR Parameterizations in the references

Reference	Cloudy-Sky Parameterization
Maykut and Church, 1973	$\mathrm{DLR}_{cld} = (0.7855 + 0.000312 \times \mathrm{CF}^{2.75})\sigma T^4$
Jacobs, 1978	$\mathrm{DLR}_{cld} = (1 + 0.26 \times \mathrm{CF})\mathrm{DLR}_{clr}$
Sugita and Brutsaert, 1993	$\mathrm{DLR}_{cld} = (1 + 0.0496 \times \mathrm{CF}^{2.45})\ \mathrm{DLR}_{clr}$
Konzelmann, 1994	$\mathrm{DLR}_{cld} = (1 - \mathrm{CF}^4)\mathrm{DLR}_{clr} + 0.954\mathrm{CF}^4\sigma T^4$

Table 5. Locally fitted cloudy-sky DLR parameterizations in TP

Reference	Locally fitted Cloudy-Sky Parameterization
Maykut and Church, 1973	$\mathrm{DLR}_{cld} = (0.85 + 0.01 \times \mathrm{CF}^3)\sigma T^4$
Jacobs, 1978	$\mathrm{DLR}_{cld} = (1 + 0.23 \times \mathrm{CF})\mathrm{DLR}_{clr}$
Sugita and Brutsaert,1993	$\mathrm{DLR}_{cld} = (1 + 0.2 \times \mathrm{CF}^{1.3})\ \mathrm{DLR}_{clr}$
Konzelmann, 1994	$\mathrm{DLR}_{cld} = (1 - \mathrm{CF}^{3.5})\mathrm{DLR}_{clr} + \mathrm{CF}^{3.5}\sigma T^4$

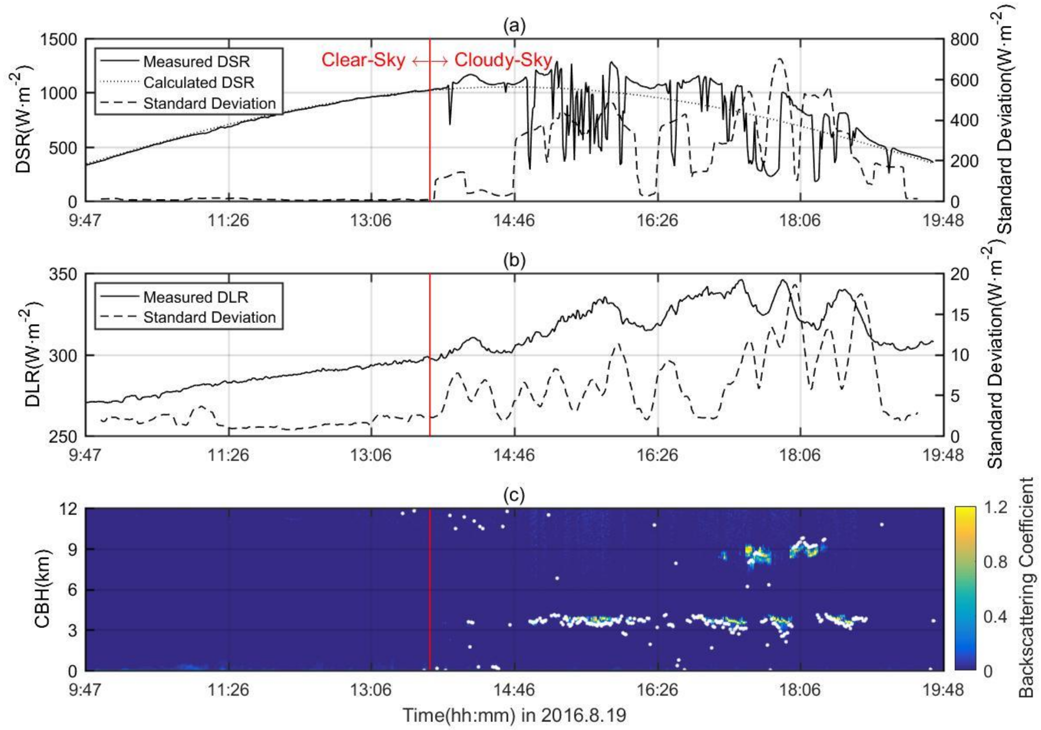

Fig. 1. Time series of data sample on 2016.8.19 transited from clear-sky to cloudy-sky: (a) measured (black line) and calculated (dotted black line) downward shortwave radiation and its 21-min standard deviation (grey line), (b) measured downward longwave radiation and 21-min standard deviation and (c) MPL backscattering coefficient and the cloud base height.

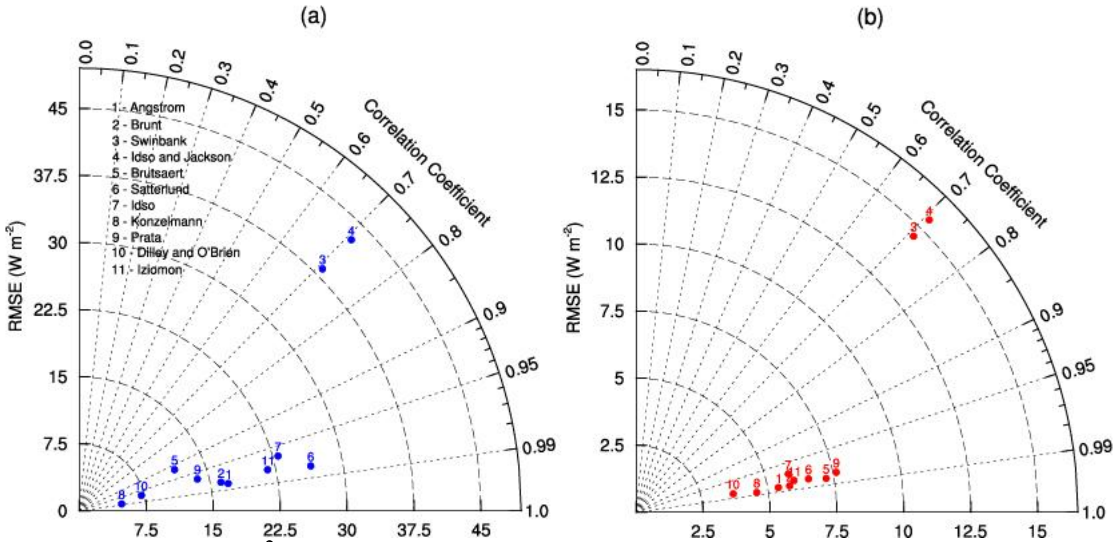

Fig. 2. RMSE and R^2 for the clear-sky DLR parameterizations using original (a) and locally calibrated (b) coefficients.

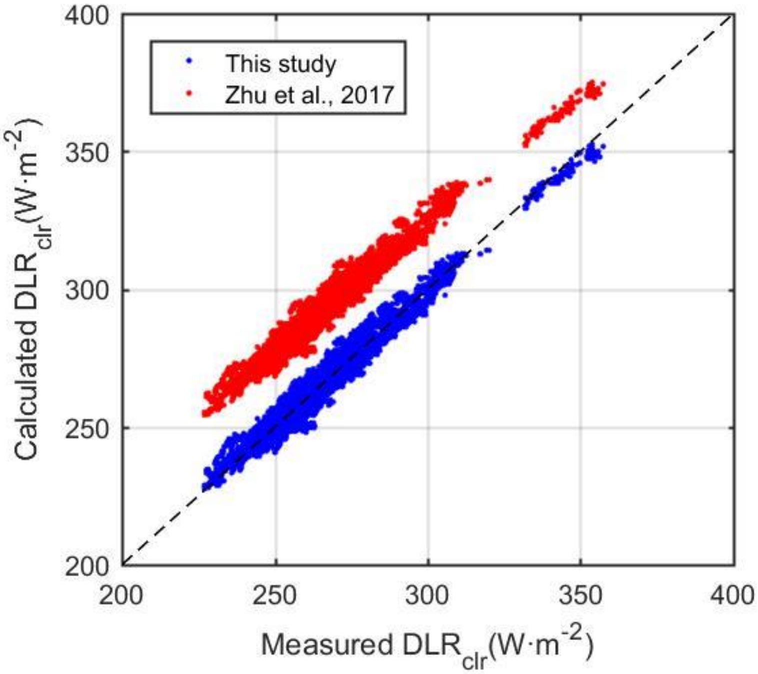

Fig. 3. Scatter plots ofmeasured clear-sky DLR data from as a function of calculations by the Eq.(3) this study (blue dots) and the Eq.(4) by Zhu et al. (2017) (red dots). The dash black line is the 1:1 line.

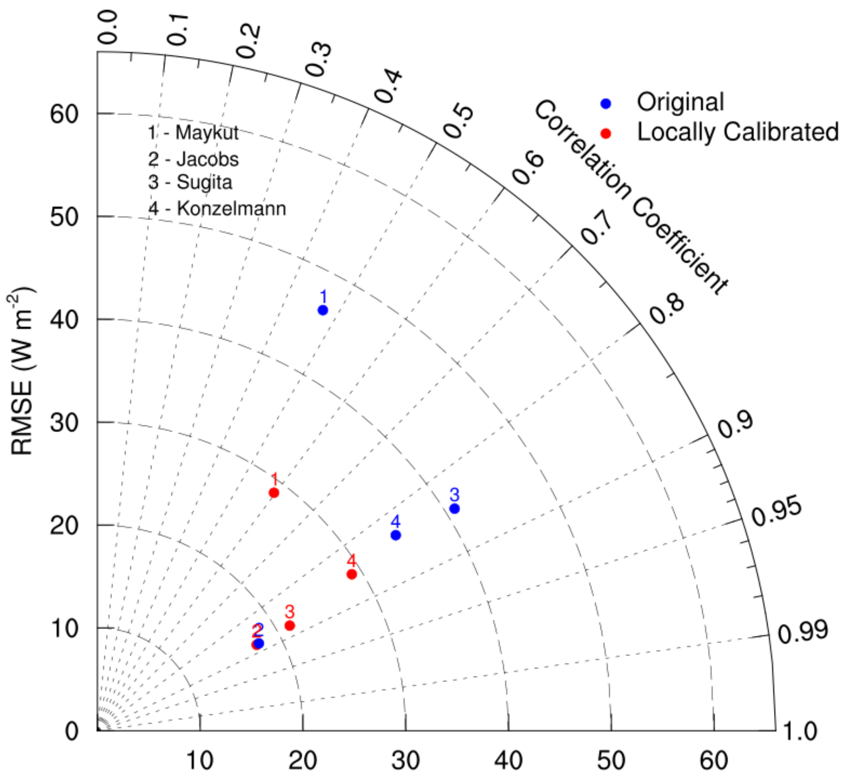

Fig. 4. RMSE and R^2 for the cloudy-sky DLR (DLR_{cld}) parameterizations using the original (blue) and locally calibrated (red) coefficient.

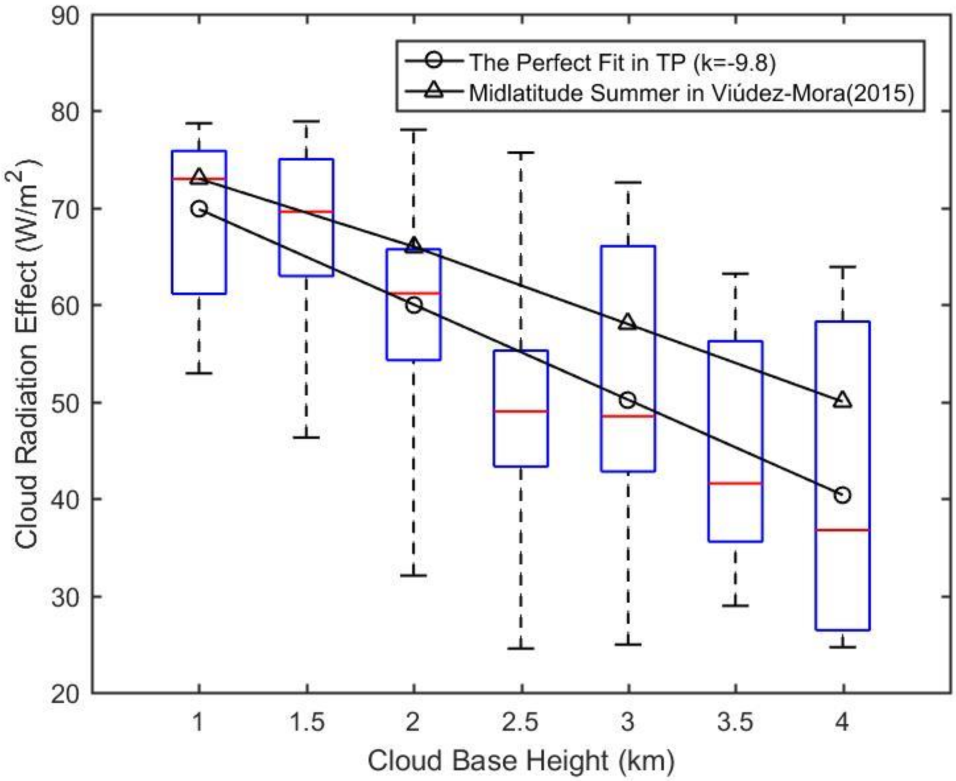

Fig. 5. Distributions of cloud radiative effect against measured cloud base height are represented by box plot (the blue box indicates the 25th and 75th percentiles, the whiskers indicate 5th and 95th percentiles, the red middle line is the median). The black circles line and the black triangles is mean values of cloud radiative effect over TP in this study and in midlatitude site (Girona, Spain) in Viúdez-Mora(2015) respectively.